Energy Storage and Conversion 2026, 4(2), 4141.
doi: https://doi.org/10.59400/esc4141

Article

Overview of integrated packaging single-cell technology for hydrogen proton exchange membrane fuel cells

Ji Pu[1,2,*], Qianya Xie[2], Kai Li[2], Zhanfeng Wang[3], Chunyu Li[3], Jun Li[4], Ziliang Zhao[5]

[1] Automotive Engineering College, Wuhan University of Technology, Wuhan 430070, China
[2] Workstation of Academician Li Jun, Foshan Xianhu Laboratory, Foshan 528234, China
[3] Automotive Engineering College, Tsinghua University, Beijing 100084, China
[4] Engine Development Department, General R&D Institute, Changchun 130013, China
[5] Transportation College, Shandong University of Science and Technology, Qingdao 266590, China
*** Corresponding author:** Ji Pu, puji@xhlab.cn

CITATION

Pu J, Xie Q, Li K, et al. Overview of integrated packaging single-cell technology for hydrogen proton exchange membrane fuel cells. Energy Storage and Conversion. 2026; 4(2): 4141. https://doi.org/10.59400/esc4141

ARTICLE INFO

Received: 9 March 2026
Revised: 28 March 2026
Accepted: 2 April 2026
Available online: 10 April 2026

Abstract: Proton exchange membrane fuel cells (PEMFCs) are gaining significant traction as a promising clean energy technology due to their high efficiency and low-temperature operation. Especially, the integrated single-cell technology is beginning to become the future trend in system applications. This paper provides a systematic review of the technological innovations and design optimizations in membrane electrodes, bipolar plates, and overall packaging for a single cell. It critically analyzes the advantages and limitations of current single-cell solutions from the perspectives of cost, performance, and durability. It points out the existing problems of traditional separate sealing, which can easily cause misalignment of the sealing components and lead to deformation of the MEA frame or even MEA tearing. The integrated packaging single-cell technology can solve these problems. It points out the existing problems of traditional separate sealing, which can easily cause misalignment of the sealing components and lead to deformation of the MEA frame or even MEA tearing. The integrated packaging single-cell technology can solve these problems. The MEA component is assembled with the anode plate and the cathode plate by using hot melt glue, and then undergoes heat curing to form a single-cell fuel cell. It also introduces the technical solutions for the inlet and outlet area, flow distribution area, distribution area, and working area of the integrated single-cell plates, as well as the structural packaging solutions for the MEA of the integrated single-cell, including single-side frame structure and double-side frame structure, pre-packaged and non-pre-packaged MEAs, and their structural and packaging processes. It provides theoretical support for the engineering application and large-scale production of PEMFC single-cell technology.

Keywords: fuel cell; single cell; packaging; high power; high temperature

1. Introduction

Fuel combustion products cause considerable damage to the environment and human health. Therefore, it is necessary to switch to environmentally friendly vehicles [1]. Hydrogen is a promising energy carrier that can achieve net-zero carbon emissions and decrease fossil fuel dependency [2]. Hydrogen energy is increasingly recognized as a pivotal, green, low-carbon, and abundant renewable resource, essential for addressing global climate change and facilitating energy transition. In March 2022, the National Development and Reform Commission and

the National Energy Administration of China successively issued the "Long-Term Development Plan for Hydrogen Energy Industry (2021–2035)", the "Action Plan for Carbon Peak Before 2030" as guiding documents for the development of the hydrogen energy industry in the next 15 years, clarifying the strategic positioning, development goals, key tasks and guarantee measures of hydrogen energy, aiming to promote the high-quality development of the hydrogen energy industry and build a diversified hydrogen application ecosystem covering transportation, energy storage, industrial production, etc. The Development and Reform Commission of Guangdong Province released the "Implementation Plan for Guangdong Province Guangzhan Hydrogen Highway Demonstration Project", promoting the construction of a hydrogen fuel cell vehicle demonstration city cluster in Guangdong Province, and exploring a large-scale commercial application model for fuel cell vehicles. Shandong, Sichuan, Henan, and Jilin provinces have implemented free policies for the highway passage of hydrogen vehicles. Various provinces have listed the development of hydrogen and fuel cell technologies as key tasks and fuel cell vehicles as key supported areas [3–7].

Fuel cell technology, as one of the key paths for the transition to clean energy, is experiencing a leapfrog development from laboratory research to large-scale commercial applications [8]. The current production process of the fuel cell stack involves welding the cathode and anode plates into bipolar plates, repeatedly stacking them with the membrane electrode assembly (MEA) in the fuel cell stack, and then applying overall pressure and sealing to form the fuel cell. This inappropriate assembly method has the following four shortcomings [9] as shown in **Table 1.**

Table 1. The shortcomings of the assembly of the traditional stack.

Shortcomings	Reason	Consequence
The relative positions of the MEA and the bipolar plate are maintained unchanged by the frictional force	The excitation from the road surface and the vehicle itself may cause the bipolar plate and the MEA to shift	Seal failure gas leakage
The laser welding of the cathode and anode plates	Damage the metal surface coating the damaged position will accelerate corrosion and aging with high potential and acidity then release ions	Reducing the insulation and performance
Sealed with silicone rubber	Low strength, high permeability, and poor acid resistance	Affecting the lifespan
Poor maintainability and low production efficiency in large-scale production	When the entire stack needs to be disassembled, the pressure between the MEA and the bipolar plate needs to be released, and then re-pressurized	Brings new sealing problems and poor uniformity between cells

Therefore, the industry generally believes that the single-cell with integrated modular packaging has many advantages, such as good sealing, convenient maintenance, high stability and reliability, and ease of large-scale production. It is the inevitable path for future fuel cells to reduce costs, improve lifespan, be commercialized, and productized. Therefore, this paper introduces the structural principle, component materials, research status, and development trends of the integrated packaging fuel cell single-cell, and points out the existing problems and solutions.

2. Overview of integrated packaging single-cell

2.1. Working principle of the integrated packing a single cell

The electrochemical working principle of the integrated packaging single-cell is identical to that of a traditional proton exchange membrane fuel cell (PEMFC). In the PEMFC, hydrogen gas at the anode and oxygen at the cathode undergo oxidation and reduction reactions, respectively, within the anode catalyst layer and the cathode catalyst layer. **Figure 1** is the working principle diagram of the PEMFC.

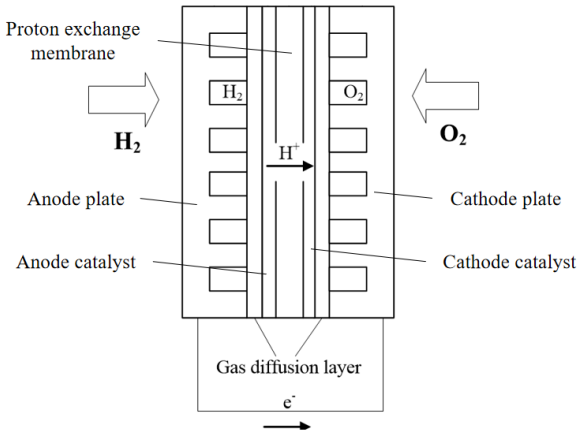

Figure 1. Working principle diagram of PEMFC.

Note: Hydrogen and oxygen pass through the plates and the gas diffusion layer to reach the catalytic layer.

When a fuel cell is operating, the gas of the cathode reaction, oxygen, enters the cathode flow channel, while the gas of the anode reaction, hydrogen, enters the anode flow channel. The gas flows through the flow channels and spreads over the surface of the fuel cell. At the same time, the gas diffuses through the gas diffusion layer (GDL) and reaches the catalytic layer (CL) to undergo electrochemical reactions. Under the action of the catalyst, it decomposes into protons and electrons. The protons pass through the proton exchange membrane to reach the cathode, and the electrons pass through the external circuit to do work and then reach the cathode, where they are collected by the current collection plate. Oxygen passes through the cathode diffusion layer to the surface of the cathode catalytic layer. Under the action of the catalyst, oxygen combines with the protons passing through the proton exchange membrane and the electrons from the external circuit to form water, releasing a large amount of heat [10–14].

2.2. Structure and components of the integrated packaging cell

The single-cell component of an integrated fuel cell is almost the same as that of the traditional PEMFC component, mainly consisting of bipolar plates, gas diffusion layers, catalytic layers, proton exchange membranes, frames, and encapsulation films. However, the structural form is different. In the traditional PEMFC stack structure, there is no independent single cell. Instead, bipolar plates and MEAs are sealed with sealing gaskets, and a certain number of bipolar plates and MEAs are stacked in series and then compressed and fastened as a whole stack by end plates with bolts or straps, as shown in **Figure 2**. Under the elastic force, the sealing gasket deforms to form

independent hydrogen and air flow channels, and the coolant flow channel is formed by integrating the cathode plate and the anode plate through welding or bonding and sealing them together. In contrast, the integrated single-cell is a standardized unit. The mainstream structure is to bond the cathode plate and the anode plate respectively to both sides of the membrane electrode through sealing films, and then encapsulate them as a whole to form an integrated packaging single-cell. The coolant flow channel is formed by adding sealing gaskets between two single cells during stacking [15–17]. This modular approach is a significant departure from the traditional method and underpins its advantages, as shown in **Figure 3**. However, its disadvantage is that it has high requirements for the production process. During the production process, the sealing glue line, bonding strength, and alignment accuracy of every single battery must all meet extremely high standards. It achieves the manufacturing efficiency and sealing reliability at the application end through strict manufacturing processes, and it is a design concept aimed at large-scale automated production.

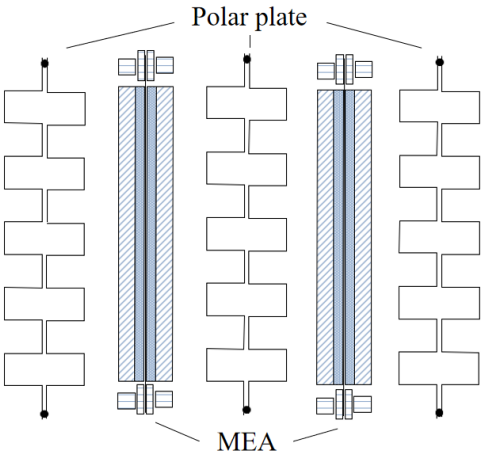

Figure 2. Traditional fuel cell stack structure (non-independent single cell structure).

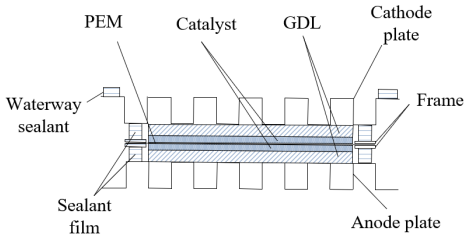

Figure 3. Structure of an Integrated Fuel Cell Single-Cell (independent single cell structure).

3. Research progress of the integrated packaging single cells

3.1. Integrated packaging single-cell sealing structure

At present, the sealing methods for fuel cells in both domestic and international markets can be mainly classified into two types: the traditional separate-sealing structure and the standardized single-cell integrated sealing. The separate-sealing method is currently the mainstream sealing method in both domestic and international markets, represented by enterprises such as Hyundai, Honda, SHPT, SunRise Power, Nowogen, and SinoFuelCell. This sealing method requires stacking multiple bipolar plates and MEA stacks and applying pressure as a whole to ensure the sealing

effect [18–22]. The most representative example of the standardized single-cell sealing method is the fuel cell installed in the Toyota Mirai II, where the MEA is bonded to the cathode and anode plates through hot melt adhesive and encapsulated as a standard hydrogen fuel single-cell. Some domestic enterprises have just started to research and develop integrated single-cell, and are currently at the stage of laboratory verification, without having mature products for application, such as H-Rise and SPIC [23–27].

The separate sealing methods are divided into the structure where the plates and sealant are integrated together, and the structure where the MEA and sealant are integrated together. Most of the stack products have an integrated structure of plates and sealant. The structure and assembly process are shown in **Figure 4**. The metal anode and cathode plates are combined through laser welding to form a bipolar plate, and the cooling side is sealed. Seals are assembled on both sides of the bipolar plate to achieve the sealing of hydrogen and air. Finally, MEA is superimposed to form a fuel cell module, and the modules are stacked according to the power requirements to assemble into a fuel cell stack. Currently, most enterprises in China, such as Shpt and SunRise Power, all adopt this sealing method.

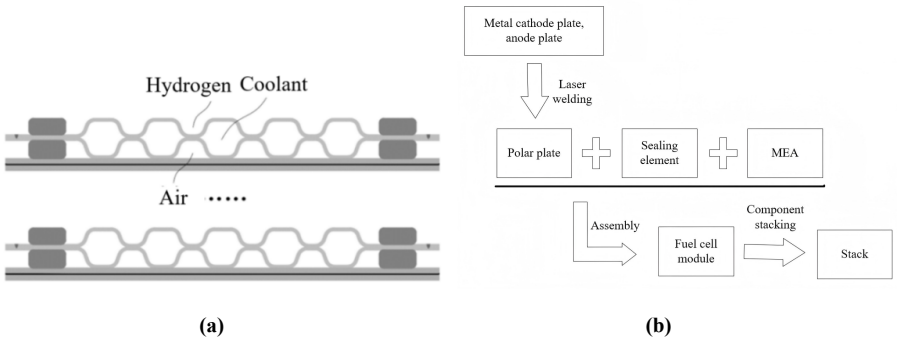

Figure 4. **(a)** The separate sealing structure; **(b)** The production process of the separate sealing structure.

This method is notoriously susceptible to misalignment during assembly, stress concentration at the MEA frame, and stringent requirements on sealing groove dimensions and compression ratios. During the assembly process, the bipolar plates, sealing components, and MEA are layered one upon another, which easily causes misalignment of the sealing components, resulting in deteriorated or even failed sealing performance. Additionally, for the stack with a separate sealing structure, the internal stress concentration usually occurs at the sealing components and the edge of the GDL. This can lead to deformation of the MEA frame and even MEA tearing. It requires optimization of the sealing component structure design to reduce stress concentration. Moreover, the sealing on the gas side needs to be achieved through the encapsulation pressure of the stack. The encapsulation pressure not only needs to ensure good sealing but also needs to guarantee the compression ratio of the GDL, which poses high requirements for the pressure control of the packaging, the size of the sealing groove structure, and the size of the sealing components. In this sealing scheme, laser welding on the cooling side will damage the corrosion-resistant coating on the surface of the metal plates, not only releasing metal ions that affect insulation but also reducing the corrosion resistance of the fuel cell. At the same time, it is not conducive to the sealing

effect on the water side, and the cost of the laser welding equipment is relatively high. Furthermore, this sealing scheme has poor maintenance convenience. If a certain cell of the stack is damaged and needs to be returned to the factory for disassembly and repair, the gas tightness of the anode and cathode flow channels may be problematic after reassembly. Moreover, the fuel cell assembled in a split structure is not a true integrated single-cell. Its structural form is not conducive to the expansion of the power of the stack [28–31].

Another type is the integrated structure of the MEA and the sealant. First, the anode and cathode plates are combined to form a bipolar plate. Then, the assembled (Catalyst Coated Membrane) CCM and GDL are placed in the mold for the injection molding of the frame. At the same time, sealing components are set on the frame. The structure and assembly process are shown in **Figure 5**. Finally, the MEA component with the sealing structure is combined with the bipolar plate to form a fuel cell, and the components are stacked to form a stack. This sealing scheme can ensure that the relative position of the sealing component and the MEA does not move, effectively avoiding misalignment caused by the layer-by-layer stacking of the sealing component and MEA, which can lead to sealing failure. This integrated structure can also avoid stress concentration at the junction between the frame and the MEA. However, this scheme requires a high-quality precision of the injection-molded sealing component molds. Since CCM, GDL, and sealant are elastic components that deform when subjected to micro-force, it is necessary to ensure precise positioning and a small relative position deviation of CCM, GDL, and sealant simultaneously. Additionally, when the MEA with the sealing structure is stacked with the bipolar plate, due to the pressure applied during assembly, the edge of the bipolar plate will slide and deform relative to the sealing component, which can also cause leakage and tearing of the MEA. This structure is not a true integrated single-cell. When a certain MEA fails, the convenience of disassembly and maintenance is the same as that of the separate sealing structure [32–34].

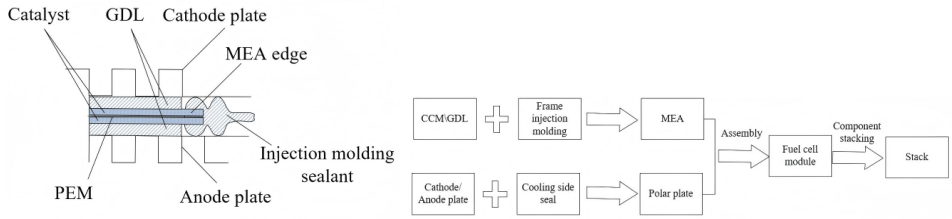

Figure 5. **(a)** Integrated structure of MEA and seal; **(b)** Production process of integrated structure of MEA and seal.

The integrated sealing approach, exemplified by Toyota's Mirai II, represents a paradigm shift. Toyota has applied this method to the fuel cell stack of its mass-produced fuel cell vehicle MiraiII. The fuel cell sealing structure and production process are shown in **Figure 6**. The assembled CCM and GDL are connected to the MEA frame through UV-curable glue, and after UV curing, the MEA component is formed. On both sides of the MEA frame, hot melt glue is pre-applied, and the MEA component, anode plate, and cathode plate with water-side sealing rubber strip injection

molded are assembled and then undergo thermal curing to form a single cell. This single cell can generate electricity independently. Compared with the previous two sealing methods, which must be combined with the next component to generate electricity, this method can expand the power range by changing the number of single cells. The use of UV glue and hot melt glue greatly improves the production speed of the single cell, and the pre-applied hot melt glue on the frame is produced using a roll-to-roll production method, significantly increasing production efficiency. The use of hot melt glue for the gas-side sealing can achieve better sealing results and does not have the problem of misalignment of the sealing parts, further improving the sealing performance. In addition, for the first two sealing schemes, if the internal of the fuel cell needs to be repaired, the sealing structure of the gas-side has undergone secondary assembly, so before leaving the factory, it is necessary to conduct a gas tightness test again; while the integrated single-cell only undergoes secondary assembly on the water-side during the repair process, and before leaving the factory, it does not need to undergo another gas tightness test, which improves the maintainability of the fuel cell [35–37].

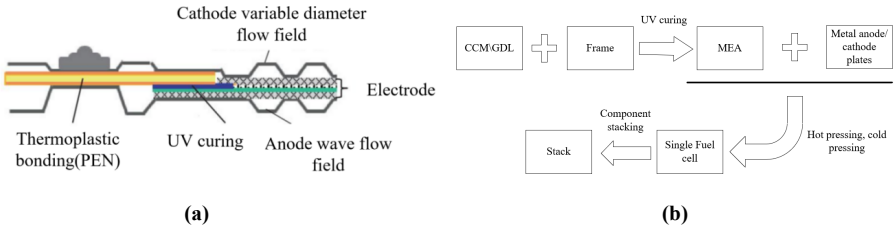

Figure 6. **(a)** Toyota integrated sealing structure; **(b)** Production process of Toyota integrated sealing structure.

However, Toyota's integrated sealing solution still has certain flaws. For instance, the heat-melt adhesive film and the Polyethylene naphthalate(PEN) resin material frame do not have elasticity, and there is a certain manufacturing tolerance in the thickness of the GDL. Compared with rubber material sealing strips or integrated resin frames, the heat-melt adhesive film cannot absorb the thickness tolerance of the GDL, causing the metal plates to deform. Additionally, during the heat-curing process of the heat-melt adhesive, due to the different curing shrinkage rates of the heat-melt adhesive film and the MEA frame, the adhesive film and the MEA frame will have different deformation amounts, resulting in a certain pulling force from the frame on the CCM and GDL components. In severe cases, it can even lead to the tearing of the proton exchange membrane.

Despite these challenges, the integrated sealing structure stands out for its production efficiency, sealing reliability, and modular potential.

3.2. Integrated packaging single-cell plate structure

The plates can be classified by function into the inlet/outlet area, the flow diversion area, the distribution area, the working flow channel area, the sealing area, the edge frame area, and the auxiliary function area. The inlet/outlet area serves as the main passage for hydrogen, air and coolant to enter and exit; the flow diversion area is the connection channel between the main passage of the reaction gas and the distribution area flow channels in each single-cell; the distribution area evenly distributes the

reaction gas to each working flow channel at the inlet and collects the reaction gas in the working flow channels to the flow diversion area at the outlet; the working flow channel area is the working area for the anode and cathode reaction gases and coolant; the sealing area is used for the installation and positioning of sealing components; the edge frame area is used for structural strength support and also serves as the positioning reference for the plate; the auxiliary area includes inspection plug-in structure, positioning structure, etc. The plate structure of the Toyota integrated packaging single-cell is shown in **Figure 7**.

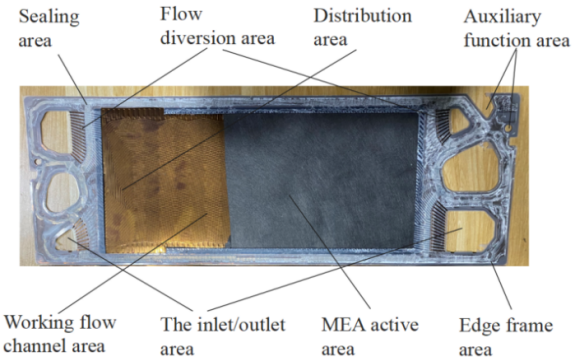

Figure 7. A structural diagram illustrating the layout of each working area of the electrode plate.

3.2.1. Inlet and outlet area

The fluid inlet and outlet include a hydrogen inlet and outlet, an air inlet and outlet, as well as a coolant inlet and outlet. The layout methods mainly include same-side layout and opposite-side layout. Generally, for an integrated sealed single-cell, a three-port same-side layout scheme is adopted because the layout method of the inlet and outlet affects the flow pattern of the fluid and the utilization rate of the plate area. The three-port same-side layout is suitable for the parallel or reverse flow of hydrogen and air. Compared with the two flow patterns, the reverse flow can enhance the activity of the chemical reaction and is more conducive to water management. The opposite side layout is suitable for the cross-flow or reverse flow of hydrogen and air. The water path is arranged on the opposite-side and crosses with the flow paths of hydrogen and air. The opposite-side layout can, to some extent, improve the uniformity of temperature distribution, but the proportion of the main inlet and outlet cross-sectional area increases, and the active area utilization rate of the entire plate decreases, thereby reducing the volumetric power density of the stack [38–41], as shown in **Figure 8**.

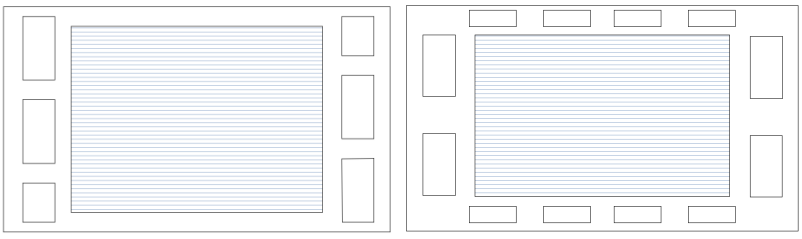

(a) **(b)**

Figure 8. **(a)** Three-port same-side layout for Inlet and Outlet Area of the medium; **(b)** Three-port opposite-side layout for Inlet and Outlet Area of the medium.

The inlet and outlet areas of the gas in the fluid affect the rate of its electrochemical reaction. The gas flow is usually calculated by decomposing the power demand of the fuel cell in the forward direction. The minimum cross-sectional area of the main inlet and outlet is determined based on the gas flow, thereby determining the shape and size of the main inlet and outlet. The specific calculation is as

$$P_{stack} = \frac{I \times V_{cell} \times N}{1{,}000}, \tag{1}$$

where P_{stack} represents stack power (kW); I represents the working current of the stack (A); V_{cell} is a cell voltage (V); N represents the number of fuel cells.

$$m_{H_2} = \frac{I \times M_1 \times N \times \tau_1}{e_1 \times F}, \tag{2}$$

where m_{H_2}represents hydrogen flow (g/s); M_1represents molar mass of hydrogen (g/mol), M_1 = 2; τ_1 represents excess coefficient of hydrogen; e_1 represents number of electrons transferred by hydrogen,e_1 = 2; F is a Faraday constant (C/mol), F = 96,485.34.

$$m_{Air} = \frac{I \times M_2 \times N \times \tau_2}{0.21 \times e_2 \times F}, \tag{3}$$

where m_{Air} represents Air flow (g/s); M_2 represents molar mass of Oxygen (g/mol), M_2 = 29; τ_2 represents excess coefficient of Oxygen; e_2 represents number of electrons transferred by Oxygen, e_2 = 4; *0.21* represents the proportion of oxygen in the air.

$$V = \frac{m \times R \times T}{P \times 1{,}000}, \tag{4}$$

where V represents volume flow rate of gas (m^3/s); m represents gas flow (g/s); R is a Universal gas constant (J $mol^{-1}K^{-1}$), R = 8.314; T represents the gas temperature, and P represents gas pressure.

$$S_{min} = \frac{V}{v} \times 1{,}000{,}000, \tag{5}$$

where S_{min} represents the minimum cross-sectional area of gas (mm^2); v represents gas velocity (m/s), Usually, hydrogen velocity is 35 m/s, air velocity is 50 m/s.

Since the volume concentration and diffusion coefficient of oxygen are much smaller than those of hydrogen, the insufficiency of oxygen will have a significant impact on the mass transfer efficiency and the rate of the electrochemical reaction. Therefore, the inlet and outlet areas of air are usually larger than those of hydrogen. The inlet and outlet areas of the coolant will affect the cooling effect. Setting the outlet area of the coolant larger than the inlet area can reduce the flow speed of the coolant and optimize the cooling effect.

3.2.2. Diversion area

Several common flow diversion Area structures are shown in **Figure 9**. The L-shaped structure is shown in **Figure 9a**, which has the simplest structure and relatively simple processing technology, and the resistance to the fluid is moderate. However, the cross-sectional area of the channel is easily affected by the changes in

packaging pressure and may get blocked or bulge. The Z-shaped structure is shown in **Figure 9b**, which is a common flow diversion method used for graphite plates and metal plates. Its sealing method is simple and effective, but the structure is relatively complex. Due to the sudden change in gas flow direction, the flow resistance of the flow diversion area is large, and compared with other structures, the utilization rate of the plate area is reduced, and there is also a problem of poor coating quality at the edge. The integrated diversion area structure is shown in **Figure 9c**, and its flow diversion area structure is integrated onto the resin frame of the MEA. The structure is relatively simple and is often used in integrated single-cell sealed structures. However, the manufacturing accuracy of the integrated resin frame is high, and the process is complex. Selecting the appropriate resin material is also a major difficulty. The straight-through patch diversion area structure is shown in **Figure 9d**. At the fluid inlet and outlet, patches containing flow diversion grooves are arranged. The fluid passes through the flow diversion grooves on the patches to enter the distribution area [42–44].

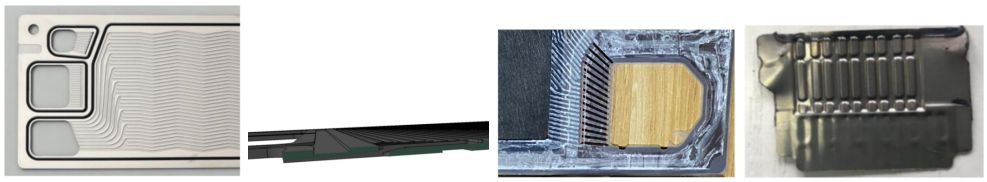

(a) **(b)** **(c)** **(d)**

Figure 9. Structure of the Diversion area: **(a)** L-shaped diversion area structure; **(b)** Z-shaped diversion area structure; **(c)** Integrated diversion area structure; **(d)** Straight-through patch diversion area structure.

Based on the above analysis, among the four structures, due to the flow channels of the integrated cell structure and the straight-through structure being straight, their flow resistance is the lowest; while the Z-shaped structure has a sudden change in structure, so the medium flow is the worst, and the flow resistance is the largest. The L-shaped structure has a moderate level of flow resistance.

3.2.3. Allocation area

The distribution area evenly distributes the fluid flowing from the diversion area into the working flow channels. The design of the distribution area directly affects the uniformity of the fluid flow and pressure distribution at the inlet and outlet of the working flow channels. The structure of the distribution area mainly includes two types: the lattice type and the linear diversion channel type. The lattice-type distribution area structure is shown in **Figure 10a**, which has a simple structure and occupies a small area, but the fluid distribution uniformity is poor and is only suitable for scenarios where the overall width of the micro-flow channels is relatively narrow. The linear diversion channel type distribution area structure is shown in **Figure 10b**, which has a more complex structure and occupies a larger area. However, by optimizing the design of the channels, the fluid distribution uniformity can be greatly improved. Generally, the linear diversion channel type distribution area structure is adopted for automotive fuel cell integrated sealed single-cells [45–47].

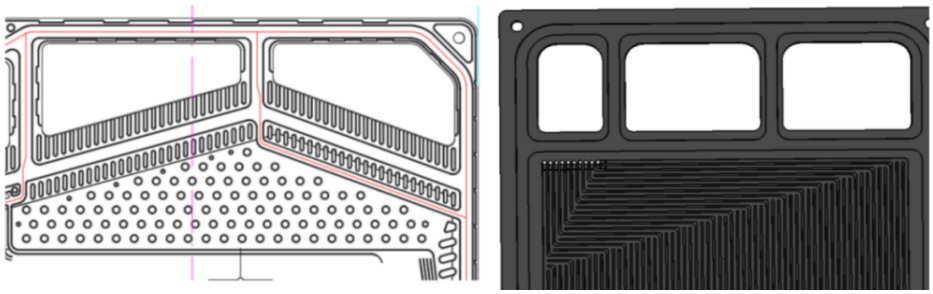

(a) (b)

Figure 10. Allocation area Structure to direct the gas into the Working flow Channel Area: **(a)** Lattice-type allocation structure; **(b)** Linear diversion channel type distribution structure.

3.2.4. Working flow channel area

The flow channel dimensions in the work flow channel area mainly concern the flow channel depth, flow channel width, ridge ratio, flow channel period, etc. Currently, the common flow channel forms mainly include parallel flow channels, serpentine flow channels, grid flow channels, cross-finger flow channels, 3D flow channels, and biomimetic flow channels. The Toyota integrated sealing single-cell work flow adopts wave-shaped flow channels and variable diameter flow channels to enhance the anode reaction effect and cathode drainage effect. The mainstream flow channels in the industry are serpentine flow channels and wave-shaped flow channels. The flow channel size and form of the bipolar plates directly determine the flow state of reactants and products in the flow channels, thereby changing the pressure drop, gas distribution uniformity, mass transfer efficiency, drainage capacity, and support strength of the bipolar plates, which will directly affect the performance and stability of PEMFC.

The structure of the sealing area has been introduced previously. In addition, the edge frame area and auxiliary structure area are almost the same as the bipolar plate structure of the traditional stack scheme, and no further introduction will be made here.

3.3. The MEA structure of integrated packaging single-cell

The MEA structure is generally designed based on the combination of the electrode plates and the sealing adhesive. It mainly consists of single-sided frame structures and double-sided frame structures, and is further divided into pre-sealed MEAs and non-pre-sealed MEAs. The single-sided frame structure is shown in **Figure 11a**, where the frame and the MEA are bonded by a hot-melt adhesive. The lengths of the gas diffusion layers on both sides and the thickness of the electrode plates are different, and the overlapping part is large. This ensures that there will be no detachment or misalignment when the pressure is applied during assembly. This scheme has a simple structure but has a difficult packaging process. The double-sided frame structure is shown in **Figure 11b**, where the two sides of the frame substrate are coated with hot-melt adhesive. One side is bonded to the MEA, and the other side is bonded to the electrode plate. The sizes of the gas diffusion layers on both sides are the same, and the thickness of the sealing area of the cathode plate and the anode plate is symmetrically designed to ensure that the compression amount of the sealing adhesive and the gas diffusion are consistent during the hot pressing process. This scheme

has a stable structure, but it is difficult to remove the adhesive from the bridge area. The pre-sealed MEA structure is shown in **Figure 11c**. After the MEA production process is completed, it is directly bonded to the traditional MEA with a baseless hot-melt adhesive and positioned, and then bonded to the two sides of the electrode plates to form a single cell. This scheme is easy to achieve automation and has a free die-cut design for the packaging area, but it has high requirements for the adhesive film sealing. The non-pre-sealed MEA is shown in **Figure 11d**. After the MEA, the sealing adhesive, cathode plate, and anode plate are stacked by a positioning device, and they are thermally pressed and sealed by a special tool to form a single cell. This scheme has a simple structure, high requirements for the accuracy of the tooling, a complex process, and is prone to risks such as misalignment and delamination [48].

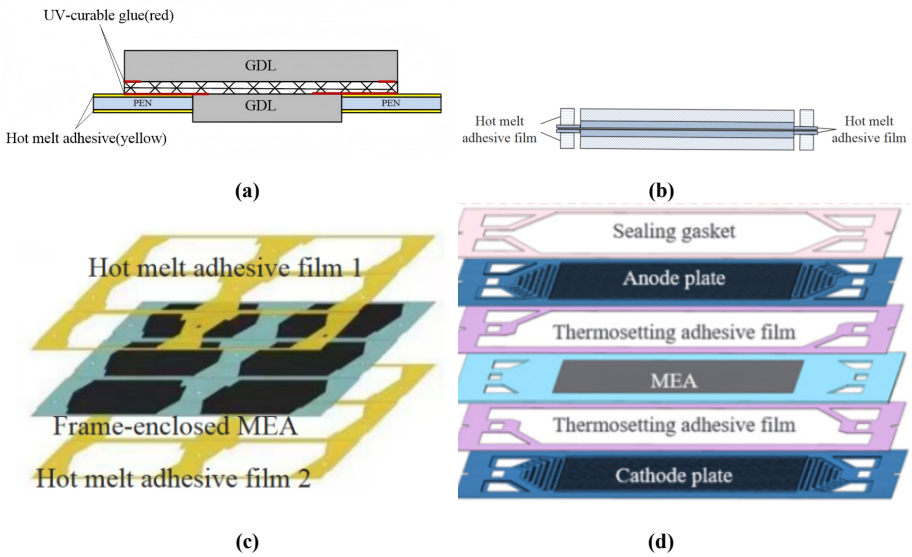

Figure 11. Integrated Sealed Single-cell MEA Structure: **(a)** Single-sided frame sealed structure; **(b)** Double-sided frame sealed structure; **(c)** The MEA structure pre-sealed by hot melt adhesive film; **(d)** Non-pre-sealed MEA structure (Sealed by the gasket).

4. Conclusion

This article summarizes the current development status of the integrated packaging single-cell for automotive fuel cells from aspects such as sealing structure, plates, flow channels, and MEAs, combined with domestic and foreign literature. It points out the existing problems of traditional separate sealing, including the stacking of bipolar plates, sealing components, and MEA during assembly, which can easily cause misalignment of the sealing components. Internal stress concentration can lead to deformation of the MEA frame or even MEA tearing. The integrated packaging single-cell technology can solve these problems. By using hot melt glue, the MEA component is assembled with the anode plate and the cathode plate with water-side sealing strips injected, and then undergoes heat curing to form a single-cell fuel cell. It also introduces the technical solutions for the inlet and outlet area, flow distribution area, distribution area, and working area of the integrated single-cell plates, as well as the structural packaging solutions for the MEA of the integrated single-cell, including single-side frame structure and double-side frame structure, pre-packaged and non-pre-packaged MEAs, and their structural and packaging processes. The

comparison between traditional fuel cells and single cells is shown in **Table 2**.

Table 2. The comparison between traditional fuel cells and single-cells.

Feature	Traditional stack	Integrated single-cell	Critical analysis
Sealing Reliability	Moderate. Relies on global compression; prone to misalignment and stress concentration.	High. Bonded sealing per cell minimizes misalignment risks and ensures independent sealing integrity.	Integrated sealing offers a fundamental improvement in reliability, which is critical for automotive vibration environments.
Manufacturing Efficiency	Lower. Sequential stacking and alignment of multiple components; laser welding can be a bottleneck.	Higher. Potential for roll-to-roll processes and pre-fabrication of standardized single-cells.	The modular nature of single-cells is inherently more compatible with automated, high-volume production.
Maintainability	Poor. Failure of one cell requires full stack disassembly, risking new issues upon reassembly.	Excellent. Individual single-cells can be replaced without disturbing adjacent cells or gas-side seals.	This is a decisive advantage for reducing lifecycle costs and improving system availability.
Scalability & Power Density	Limited by stacking height and uniformity issues; increasing cell count reduces reliability.	High. Multi-unit designs enable large active areas within a single cell, improving volumetric power density.	Integrated single-cells enable a more robust path to high power without the penalties of excessive part count.
Cost Potential	High part count and complex assembly lead to higher costs at lower volumes.	Lower part count and streamlined assembly have the potential for significant cost reduction at scale.	While initial costs may be high, the integrated approach has a steeper learning curve and greater potential for cost reduction.

At the same time, it points out that as fuel cells are developing towards higher power and productization, the multi-unit large active area single-cell technology for automotive and the high-temperature MEA technology for automotive will become new technical development directions.

Author contributions: Every author played a significant role at various stages of the research process, culminating in the final report as detailed below. Conceptualization, JP and QX; methodology, JP; validation, ZW and CL; formal analysis, JP; investigation, KL; resources, JL and ZZ; data curation, QX; writing—original draft preparation, JP; writing—review and editing, JP and QX; visualization, JP and QX; supervision, JP and QX; project administration, KL; funding acquisition, JL. All authors have read and agreed to the published version of the manuscript.

Funding: This research was funded by the Department of Science and Technology of Jilin Province, grant number NO. 20240301005ZD.

Institutional review board statement: Not applicable.

Informed consent statement: Not applicable.

Data availability statement: No new data were created.

Acknowledgment: The authors acknowledge the support from Xianhu Laboratory in Foshan. Special thanks to Academician Li Jun for his guidance on the research of large active area fuel cell single-cells. The authors would like to acknowledge the contribution of Wang Zhanfeng and Li Chunyu in the design of the sealing technology and manufacturing process in this study.

Conflict of interest: The authors declare no conflict of interest.

AI use statement: The authors declare that no artificial intelligence (AI) tools were used in the preparation of this manuscript.

References

1. Koval V, Shmygol N, Đurović S, et al. Analysis of Innovative Electromobility Development and the Advancement of Eco-Friendly Transport Infrastructure. Sustainability. 2025; 17(3): 1010. doi: 10.3390/su17031010
2. Sezer MD, Ada E, Kazancoglu Y. Investigating the Key Drivers in the Transition to Sustainable Hydrogen Transportation Fuel. Economics Ecology Socium. 2024; 8(3): 16–26. doi: 10.61954/2616-7107/2024.8.3-2
3. Rezk H, Ghasemi M, Al Saadi A, et al. Experimental validation of single and multi-objective optimization of microbial fuel cell based on recent electric eel foraging algorithm. Energy. 2025; 339: 138989. doi: 10.1016/j.energy.2025.138989
4. Rocha C, Knöri T, Ribeirinha P, et al. A review on flow field design for proton exchange membrane fuel cells: Challenges to increase the active area for MW applications. Renewable and Sustainable Energy Reviews. 2024; 192: 114198. doi: 10.1016/j.rser.2023.114198
5. Sheng B, Zeng Q, Li Y, et al. Research progress for single component fuel cell. Acta Materiae Compositae Sinica. 2025; 42(5): 2430–2441. Available online: https://fhclxb.buaa.edu.cn/en/article/doi/10.13801/j.cnki.fhclxb.20240914.002 (in Chinese)
6. Fan L, Tu Z, Chan SH. Recent development of hydrogen and fuel cell technologies: A review. Energy Reports. 2021; 7: 8421–8446. doi: 10.1016/j.egyr.2021.08.003
7. Gao WT, Lei, YJ, Zhang X, et al. An overview of proton exchange membrane fuel cell. Chemical Industry Progress. Chemical Industry and Engineering Progress. 2022; 41(3): 1539–1555. (in Chinese)
8. Mounika K, Bhattacharjee A. Design and experimental validation for performance analysis of non-isolated power converter topologies in fuel cell integrated dynamic load based local energy systems. Energy. 2025; 322: 135576. doi: 10.1016/j.energy.2025.135576
9. Krastev VK, Baldelli M, Bartolucci L, et al. Optimal cathode design of a single high temperature PEM fuel cell: A computational study. International Journal of Hydrogen Energy. 2025; 142: 80–89. doi: 10.1016/j.ijhydene.2025.05.346
10. Datta R. Fuel Cell Principles, Components, and Assemblies. John Wiley & Sons; 2014.
11. Jiang JY, Zhang Y, He XW, et al. Working principle of microbial fuel cell and strategies for enhancing power generation performance. Journal of Environmental Engineering Technology. 2024; 14(2): 699–709. Available online: https://www.hjgcjsxb.org.cn/en/article/Y2024/I2/699 (in Chinese)
12. Nair AN, Lal S, Vangala SPK. Understanding the Impact of Flow Fields on the Performance of Direct Methanol Fuel Cells: A Review on Design Trends. The Chemical Record. 2025; 25(11): e202500025. doi: 10.1002/tcr.202500025
13. Eikerling M, Kulikovsky A. Polymer Electrolyte Fuel Cells. CRC Press; 2014. doi: 10.1201/b17429
14. Wang WZ, Pei FL, Shi L. Research on Contact Pressure Distribution of Proton Exchange Membrane Fuel Cell Single Cell. Automotive and New Power Sources. 2024; 7(6): 68–74. (in Chinese)
15. Wen XF, Chen ZT, Zhan ZG, et al. Vibration response analysis of proton exchange membrane fuel cell based on finite element method. Chinese Journal of Power Sources. 2022; (8): 903–906. (in Chinese)
16. Zhou H, Liu ZE, Li YC, et al. Study on the Impact of Defective Single Cell on the Performance of Vehicular Proton Exchange Membrane Fuel Cell. Automotive Engineering. 2023; 45(10): 1876–1884. (in Chinese)
17. Jiao K, Xuan J, Du Q, et al. Designing the next generation of proton-exchange membrane fuel cells. Nature. 2021; 595(7867): 361–369. doi: 10.1038/s41586-021-03482-7
18. Yuan XZ, Nayoze-Coynel C, Shaigan N, et al. A review of functions, attributes, properties and measurements for the quality control of proton exchange membrane fuel cell components. Journal of Power Sources. 2021; 491: 229540. doi: 10.1016/j.jpowsour.2021.229540
19. Shi D, Cai L, Zhang C, et al. Fabrication methods, structure design and durability analysis of advanced sealing materials in proton exchange membrane fuel cells. Chemical Engineering Journal. 2023; 454: 139995. doi: 10.1016/j.cej.2022.139995
20. Ye D, Zhan Z. A review on the sealing structures of membrane electrode assembly of proton exchange membrane fuel cells. Journal of Power Sources. 2013; 231: 285–292. doi: 10.1016/j.jpowsour.2013.01.009
21. Dong WY, Pan JX, Guo W. Study on Reverse Polarization of Proton Exchange Membrane Fuel Cell Stack Caused by Anode Starvation. Journal of Higher Education Chemistry. 2024; 45(2): 20230397. (in Chinese)
22. Zhou Y, Gao X, Wang L, et al. Integrating ion-electron dual conducting single atom catalyst for Alkaline Anion Exchange Membrane Fuel Cell. Chemical Engineering Journal. 2025; 516: 164103. doi: 10.1016/j.cej.2025.164103

23. Sun SD, Li Z, Yuan BF, et al. Design and operation characteristics study of integrated coal gasification fuel cell power generation and methanol cogeneration system. Clean Coal Technology. 2023; 29(3): 49–55. Available online: https://www.jjmjs.com.cn/article/doi/10.13226/j.issn.1006-6772.H23031101 (in Chinese)
24. Habibnia M, Shakeri M, Nourouzi S. Determination of the effective parameters on the fuel cell efficiency, based on sealing behavior of the system. International Journal of Hydrogen Energy. 2016; 41(40): 18147–18156. doi: 10.1016/j.ijhydene.2016.06.258
25. Zhang Q. Research on the Superelastic Constitutive Relationship of Hydrogen Fuel Cell Sealing Composite Materials and Optimization of Sealing Structure [PhD Thesis]. Beijing University of Chemical Technology; 2022. (in Chinese)
26. Yin J, Yang F, Yang DJ, et al. Integrated Sealing Design and Simulation of Proton Exchange Membrane Fuel Cell. Automotive Technology. 2021; 11: 15–21. (in Chinese)
27. Liao S, Qiu D, Yi P, et al. Optimization design of assembly sequence for the proton exchange membrane fuel cell stacks with dimensional errors. Proceedings of the Institution of Mechanical Engineers, Part B: Journal of Engineering Manufacture. 2025; 239(13): 1869–1882. doi: 10.1177/09544054241290929
28. Qiu D, Peng L, Yi P, et al. Review on proton exchange membrane fuel cell stack assembly: Quality evaluation, assembly method, contact behavior and process design. Renewable and Sustainable Energy Reviews. 2021; 152: 111660. doi: 10.1016/j.rser.2021.111660
29. Yoshizumi T, Kubo H, Okumura M. Development of High-Performance FC Stack for the New MIRAI. In: Proceedings of the SAE WCX Digital Summit; 6 April 2021; Pennsylvania, PA, US. doi: 10.4271/2021-01-0740
30. Toyota Motor Corporation. Single Cell Battery for Fuel Cell. 201710433004.2, 19 December 2017.
31. Zhao J, Guo H, Ping S, et al. Research on Design and Optimization of Large Metal Bipolar Plate Sealing for Proton Exchange Membrane Fuel Cells. Sustainability. 2023; 15(15): 12002. doi: 10.3390/su151512002
32. Chan AL, Yu H, Reeves KS, et al. Identifying electrochemical processes by distribution of relaxation times in proton exchange membrane electrolyzers. Journal of Power Sources. 2025; 628: 235850. doi: 10.1016/j.jpowsour.2024.235850
33. Chen J, Goshtasbi A, Soleymani AP, et al. Effects of cycle duration and test hardware in relative humidity cycling of a polymer electrolyte membrane. Journal of Power Sources. 2020; 476: 228576. doi: 10.1016/j.jpowsour.2020.228576
34. Mizuno S, Hayashi T, Kubo H, et al. Development of the Fuel Cell Stack for the Second-Generation Mirai. TOYOTA Technical Review. 2021; 66: 22–27. Available online: https://global.toyota/pages/global_toyota/mobility/technology/toyota-technical-review/TTR_Vol66_E.pdf
35. Nagasawa T, Nogi A, Ikeda T, et al. Production Engineering Technology for the Fuel Cell Stack of the Second-Generation Mirai. TOYOTA Technical Review. 2021; 66: 34–39. Available online: https://global.toyota/pages/global_toyota/mobility/technology/toyota-technical-review/TTR_Vol66_E.pdf
36. Toyota Motor Corporation. Fuel Cell and Its Manufacturing Method. 202011313036.7, 28 May 2021.
37. Morin A, Xu F, Gebel G, et al. Influence of PEMFC gas flow configuration on performance and water distribution studied by SANS: Evidence of the effect of gravity. International Journal of Hydrogen Energy. 2011; 36(4): 3096–3109. doi: 10.1016/j.ijhydene.2010.11.070
38. Gong C, Tu Z, Xu Y, et al. Optimization Design of Geometric Parameters for Solid Oxide Fuel Cell Single Cell Flow Field. Journal of Physics: Conference Series. 2025; 3015(1): 012020. doi: 10.1088/1742-6596/3015/1/012020
39. Zhang Z, Liu H, Lan G, et al. Single-cell modeling, simulation and optimization of high-temperature proton exchange membrane fuel cells: current status, challenges, and perspectives. Journal of Power Sources. 2026; 664: 238943. doi: 10.1016/j.jpowsour.2025.238943
40. Zhang S, Ren H, Fang H, et al. Design of flow field structure and three-dimensional multiphase flow simulation for bipolar plates in the proton exchange membrane fuel cell: A novel bio-inspired conjugate dual-channel serpentine flow path. Fuel. 2026; 405: 136675. doi: 10.1016/j.fuel.2025.136675
41. Ose N, Sato K. Gas separator for fuel cells and fuel cell equipped with gas separator. US8518601B2, 27 August 2013.
42. Zhao Y, Peng L. Formability and flow channel design for thin metallic bipolar plates in PEM fuel cells: Modeling. International Journal of Energy Research. 2019; 43(7): 2592–2604. doi: 10.1002/er.4226
43. Zhong D, Lin R, Liu D, et al. Structure optimization of anode parallel flow field for local starvation of proton exchange membrane fuel cell. Journal of Power Sources. 2018; 403: 1–10. doi: 10.1016/j.jpowsour.2018.09.067
44. Shanghai ZHIZHEN New Energy Equipment Co., Ltd. A New Inlet Structure for Metal Bipolar Plates of Fuel Cells. 201910900150.0, 23 September 2019.
45. Dayan A, Azizi K, Cleemann LN, et al. Dibromoxylene-crosslinked sulfonated para-PBI membranes for use in high temperature polymer electrolyte membrane fuel cells operating with reformate gas. Electrochimica Acta. 2025; 514:

145630. doi: 10.1016/j.electacta.2024.145630
46. Indicatti FI, Rädler M, Stammen E, et al. Optimizing adhesive rheology for stencil printing of fuel cell sealings using supervised machine learning. International Journal of Adhesion and Adhesives. 2024; 132: 103693. doi: 10.1016/j.ijadhadh.2024.103693
47. Lafforgue C, Toudret P, Micoud F, et al. Manufacturing of carbon-supported platinum cathodes for proton exchange membrane fuel cell using the doctor blade process: Microstructure and performance. Journal of Power Sources. 2025; 627: 235851. doi: 10.1016/j.jpowsour.2024.235851
48. Liu YC, Lin CH, Chen S, et al. Enhancing the power density and durability of polymer electrolyte membrane fuel cells based on pulsed laser deposition-prepared Pt catalyst layer by using a nanoporous CeO2 overlayer and drop-casted Nafion with optimized drying condition. International Journal of Hydrogen Energy. 2025; 98: 242–253. doi: 10.1016/j.ijhydene.2024.12.086